Hindawi
Advances in Civil Engineering
Volume 2023, Article ID 7738042, 15 pages
https://doi.org/10.1155/2023/7738042

Research Article

Analysis of Influence of Ultra-High Pressure Water Jet Cutting Pressure Sequence on Pressure Relief and Reflection Improvement of Coal Seam

Shoulong Ma [1,2]

[1]*School of Civil Engineering and Architecture, Anhui University of Science and Technology, Huainan, Anhui 232001, China*
[2]*China Coal Xinji Energy Co., Ltd., Huainan, Anhui 232001, China*

Correspondence should be addressed to Shoulong Ma; 2020100046@aust.edu.cn

Received 15 October 2022; Revised 6 November 2022; Accepted 23 February 2023; Published 1 April 2023

Academic Editor: Zhuo Chen

In order to explore the pressure relief effect of the two combined pressure relief and antireflection technologies of ultra-high pressure water jet cutting before pressure and pressure before cutting, theoretical analysis, numerical simulation, and field test were used to study the main control factors of the combined high-pressure water jet slit cutting and fracturing antireflection technology. This paper introduces the combined technology of ultra-high pressure hydraulic fracturing, and analyses the mechanism of pressure relief and transparency enhancement of the combination of cutting before pressure and pressure relief after cutting. The results show that the starting pressure of the coal seam with ultra-high pressure water jet cutting and pressure relief is 13 MPa, the influence radius of hydraulic fracturing is 45–55 m, the starting pressure of the coal seam with pressure cutting and pressure relief is 16 MPa, and the influence radius of hydraulic fracturing is 35–45 m. Compared with pressure cutting combined pressure relief and permeability enhancement technology, cutting pressure relief and permeability enhancement technology can improve the permeability of coal seams more evenly and effectively, and reduce the stress of coal seams near the hole. The ultra-high pressure cutting and pressure combined technology can make the pressure relief of coal body uniform and sufficient, and the overall permeability coefficient of the coal body is greatly improved. The drilling purity is 2.3 times of the extraction purity of the ordinary single hole drilling, and the extraction influence range is increased, and the extraction effect is significantly improved. At the same time, the stress of coal body is reduced after slitting, and the starting pressure of hydraulic fracturing is reduced. The research results provide a scientific basis for the coal seam pressure relief and permeability enhancement under similar conditions in the mining area and have a broad application prospect.

1. Introduction

At present, there are more than 2000 coal and gas outburst, rock burst, and high gas mines in China, accounting for 30% of the total number of mines. After entering deep mining, the problems of high gas and high ground stress are prominent, the permeability of coal seam is reduced, and the difficulty of disaster management is increased [1–3]. Under the condition of deep mining, the coal seam is upgraded to the protruding coal seam. For the protruding coal seam without protective layer mining or first mining, the anti-protruding measures in the prepumping area of dense conventional borehole are still the main measures. In order to achieve efficient control of gas disasters in deep mines, the conventional pressure relief and reflection improvement technologies in coal mines in China at the present stage mainly include hydraulic punching, hydraulic cutting, hydraulic fracturing, and deep-hole presplitting blasting [4–6].

Although the deep-hole presplit blasting technology can significantly improve the pressure relief and antireflection effect of coal seam, it is relatively less applied in the pressure relief and antireflection improvement of coal seam, because the long borehole coal seam is prone to collapse, resulting in charging difficulties, and it is difficult to eliminate the risk of misfiring and explosion refusal in blasting operation. In recent years, the reflection improvement technology of

hydraulic coal seam in China has entered a stage of rapid development. The individual technology is constantly improved, and the overall development is in the direction of integration and diversification. The hydraulic measures such as low-pressure hydraulic punching, hydraulic cavitation, hydraulic fracturing, and hydraulic slotting have become the hot spots of research in scientific research institutions, which provide support for the control of coal mine gas disasters and have achieved results under certain conditions [7–10]. The hydraulic technology is often used in the field, and the hydraulic punching pressure is generally 5–20 MPa, which has a certain effect on the pressure relief and reflection improvement of soft coal seam, while the hydraulic punching efficiency of medium and hard coal seam is low. However, it is difficult to control the shape of punching holes in soft coal seam, and the amount of slag is not uniform, so there may be hole collapse, hole injection, or roadway gas overlimit during operation. The hydraulic fracturing has a large influence range and good antireflection effect, and is mostly used in medium and hard coal seams. However, it is difficult to control the fracture propagation direction in the coal body [11–13]. Hydraulic cutting seam technology is based on high-pressure water cutting technology of coal seam, improve coal seam gas flow state, reduce the stress, can effectively prevent coal, and gas outburst and the impact of ground pressure disasters happen, suitable for high ground stress, gas and low permeability coal seam (seam hardness $f > 0.4$) bedding face drilling, wear layer drilling, and shimen uncovering coal unloading antireflection and so on [14–16].

The ultra-high pressure water jet cuts the coal body, and the coal body around the slot produces deformation space so that the coal body around the slot can be fully depressurized. At the same time, because a part of the coal body around the drill hole is transported out of the drill hole by the water jet, a large number of cracks are generated in the expansion and deformation of the coal rock, changing the permeability conditions of the coal rock. Ge et al. established a fluid-solid coupling gas drainage model of slotted borehole. Through numerical simulation analysis, it is believed that the influence radius of the borehole drainage after hydraulic slotting has a power function relationship with slot disc, permeability, drainage time, gas pressure, and other factors. Through model research, it is determined that the influence significance of each factor from large to small is permeability, drainage time, gas pressure, and slotting depth [17]. Li et al. used a dynamic damage model to study the cutting process of soft coal rock by water jet. During the cutting process, with the gradual release of stress around the slot, the crack continued to expand in some directions. The tension and shear fractures in coal and rock continue to develop during the damage accumulation process, in which short pulses with high peak stress can form relatively short fractures, and long pulses with low peak stress can form relatively long fractures. Under the continuous action, the cracks around the slot cut by the jet gradually develop and then connect to each other to form a breakthrough failure [18]. Tang et al. conducted numerical simulation on the influence of different hydraulic slotting arrangements on the coal seam pressure relief and outburst prevention, and analyzed the influence of parallel, diamond, and staggered pressure relief. The results show that the coal rock pressure relief effect above the fracture groove is most obvious. The results showed that the pressure relief effect of coal and rock above the slot was the most obvious [19]. Through indirect measurement of gas flow through similar material test, it is confirmed that the pressure relief of coal seam has a significant impact on permeability, and the permeability coefficient of coal and rock increases synchronously with the degree of pressure relief. By studying the displacement and stress changes of coal body under different slit widths after high-pressure water jet slotting, the influence of slit depth on coal rock disturbance is analyzed. Numerical simulation shows that the pressure relief range of 1.0 m, 1.5 m, and 2.0 m slotting on coal body reaches 2.6 m, 3.8 m, and 5.0 m, and the influence range of slit on coal body increases with the increase of slit width. The larger the slit depth is, the more conducive to coal seam pressure relief.

The antireflection technology of hydraulic fracturing was first used in the exploitation of oil and gas fields, as a main measure of oil and gas well stimulation. In the 1960s, the hydraulic fracturing technology began to be used in coal mines to increase in coal seam permeability, mainly by drilling deep into the coal body through injection of high-pressure water, and fracturing the coal body with water as the energy transmission medium. After high-pressure water fracturing, the stress of surrounding coal body was reduced, and the stress concentration was transferred to the depth of the coal body, thus improving the permeability of coal body around the borehole, providing a good condition for drilling gas extraction [12, 20–22]. The research on the hydraulic fracturing technology in coal mine mainly focuses on the theoretical research on the initiation and extension laws of the hydraulic fractures, or the establishment of hydraulic fracturing mathematical model for numerical calculation research, or the physical experiment research of hydraulic fracturing in the laboratory. Hubbert and Willis described the stress distribution law of hydraulic fracturing wall and surrounding coal and rock mass based on classical elastic mechanics, and thus obtained the theoretical calculation model of tensile failure fracture pressure of coal and rock mass: $P_b = 3\sigma_{\min} - \sigma_{\max} + f_t$ ($\sigma_{\min}$, $\sigma_{\max}$, and f_t are the minimum horizontal stress, the maximum horizontal stress, and the tensile strength of coal rock, respectively); the comprehensive effects of the tangential principal stress σ_θ, straight principal stress σ_v, and radial principal stress σ_r on the wall of the borehole are not fully considered in this theory [23]. Ma et al. conducted an experimental study on the influence of water pressure with different water flow rates on the fracture initiation characteristics of coal. The results show that the increase in water flow rate makes the fracture morphology more complex, and the research results have important theoretical significance for revealing the fracture initiation behavior of boreholes [24]. According to the first strength criterion, Lv deduced the critical value calculation formula of pressure crack initiation pressure and successfully tried it in Pingmei Ten Mine [25]. Bouteca developed a full 3D morphological mathematical model of hydraulic fracturing

by combining the 3D spatial fluid flow field model with the elliptical fracture deformation model of Shah and Kobagashi [26]. Based on the fluid-solid interaction theory, Lian et al. analyzed the problem of hydraulic fracture propagation, took the critical stress as the criterion of the fracture initiation and extension, deduced the pressure drop equation expression in the fracture wall, and established the calculation model. ABAQUS software was used to simulate the influence of surrounding rock stress, rock mechanical properties, fracturing fluid seepage characteristics, and other external factors on hydraulic fracture propagation [27]. Bjerrum et al. carried out hydraulic fracturing tests by injecting high-pressure water into a small circular tube at the bottom of the fracturing sample in a triaxial pressure test device, and concluded that the propagation direction of hydraulic fractures was generated along the minimum principal stress surface [28]. Chen et al. used the true triaxial test device to conduct AE monitoring on the fracture of raw coal samples under fracturing. The research results can reveal the source characteristics of the whole fracture process of raw coal samples in the true triaxial hydraulic fracturing process, and evaluate the safety of the fracture process [29]. Deng et al. studied the control parameters of hydraulic crack propagation behavior by the method of hydraulic fracturing under the control of ground stress field, and conducted a systematic experimental study on the relationship between the formation and expansion of hydraulic crack and the change of coal permeability and the action of hydraulic pressure. The research results have practical significance for improving the design effect of top coal precracking [30]. Liu et al. studied the internal microstructure evolution mechanism of different coals under liquid nitrogen cooling. The experimental results show that the total pore volume and pore surface area of coal are increased after cold leaching, the heterogeneity of pore structure is enhanced, the fractal dimension is increased, and the development of porous structure of coal is promoted by cold leaching [31]. Zhou et al. took Longhu coal mine in Qitaihe mining area as the research object to study the stability of roadway floor heave. The new support scheme is adopted to reduce the floor heave of roadway by 81%. The research results can provide guidance for the optimization of roadway support [32]. Surrounding rock control and support stability of super high mining face was studied by Wang Sheng. The results of this study can provide guidance for the selection of scaffolds and the adoption of measures to improve the stability of scaffolds when they are used in ultra-high height conditions [33]. Taking Linyi mining area as the research object, Li Xuelong studied the distribution law of ground stress in deep mines. It is found that the relationship between principal stresses is $\sigma(H) > \sigma(v) > \sigma(h)$, which belongs to the strike-slip stress system. Under this stress condition, the soil lateral pressure coefficients are all greater than 1, and the magnitude of the three principal stresses increases with the increase in depth. The research results have certain reference significance for mine disaster prevention and safety production [34]. Liu Haiyan studied the failure mechanism and control technology of cave-side stoping roadway in close distance coal seam. It is proposed that *U*-shaped steel telescopic support erection and backwall filling are used to control the surrounding rock of goaf mining in the process of roadway excavation, and the on-site monitoring results also meet the engineering requirements. The research results can provide guidance for roadway design of goaf under similar mining geological conditions [35–51].

The application of ultra-high pressure hydraulic slotting technology can realize the precise seam cutting, rapid pressure relief, and efficient permeability increase, and drilling engineering quantity is reduced on the basis of the extraction standard time to shorten 30% of the effect. With the application of hydraulic fracturing technology, the impact area of hydraulic fracturing is more than 50 m, with a large impact area and obvious antireflection effect in the region. After the application of ultra-high pressure hydraulic slit technology and hydraulic fracturing technology, the antireflection effect of coal seam is remarkable. Therefore, in the hydraulic cutting seam technology and hydraulic fracturing technology in the application process, there exist the following problems: the super high-pressure hydraulic cutting seam to improve the unloading antireflection effect at the same time, greatly reduce drilling of quantities, as local antireflection measures that it is obvious, but for large area still needs to undertake a large number of slotted drilling construction slot unloading antireflection. Although the antireflection effect of hydraulic fracturing technology has a large influence range, it is difficult to control the fracture propagation direction in the coal body, and the pressure relief and antireflection improvement are not uniform, and there is stress concentration phenomenon.

To sum up, to better carry out uniform permeability improvement in low permeability coal seam, accurately control the pressure relief and permeability improvement area, greatly reduce the drilling engineering quantity, and solve the technical problems of gas extraction and control in low permeability coal seam. The combined technology of ultra-high pressure hydraulic slit cutting and hydraulic fracturing is explored, and the mechanism of pressure relief and reflection improvement by cutting and pressure relief and cutting is analyzed. The hydraulic cutting pressure scientific model is established, and the influence range of high pressure hydraulic cutting pressure is solved through theoretical analysis. The PFC software based on the theory of discontinuous media mechanics was used to simulate the initiation and expansion characteristics of seam cutting and fracturing fractures in coal seam, and the distribution rules of fractures and stresses in coal seam were compared and analyzed by hydraulic cutting before pressure and pressure relief after cutting. Combined with the field research on ultra-high pressure hydraulic cutting before pressure and pressure before cutting and combined pressure before cutting and permeability improvement, the influence law of ultra-high pressure water jet cutting pressure sequence on pressure relief and permeability improvement of coal seam is further revealed. The research results are of great significance to enrich the comprehensive gas control technology of low permeability coal seam.

2. Ultra-High Pressure Hydraulics First Cut and Then Pressure Combined with the Principle of Permeation

The concept of hydraulics first cut and then pressurized joint mode is to use ultra-high pressure hydraulic cuts to cut the coal seam in the coal seam first, and then use hydraulic fracturing to fracturing the coal seam after the gap is generated. The groove generated by the hydraulic cutting in the early stage can guide the hydraulic fracturing so that the extension direction of the fracture in the plastic zone is basically the same as the direction of cracking. The crack expansion is more uniform.

By forming a slot by hydraulic cutting in the coal body in advance, the effective influence range of the single hole can be expanded to a certain extent. The original stress balance of the coal body can be destroyed. The coal body around the cut hole is transported to the space of the slot space, and the pressure relief, deformation, and expansion of the coal seam can occur, further generating more cracks and expanding the plastic area of the coal body near the cut hole. Combined with the empirical formula of plastic theory, it can be seen that the radius of the plastic zone is about 3 to 5 times the radius of the cut groove, and the radius of the high-pressure water groove is determined to be about 2.5 m through field tests. It is inferred that the radial plastic zone range outside the hydraulic groove is about 7.5 to 12.5 m. After the hydraulic cut is formed into a crevice, a weak surface is generated in the drilling hole, and after the fracturing water enters the crack, it promotes the cracking, expansion, and extension of the weak side crack, resulting in the full and uniform development of the coal body fracture near the borehole. Through the rational arrangement of the cut-pressure joint hole, a three-dimensional fracture network of interpenetration is formed between the drilled holes, which effectively solve the problems of disorderly expansion of the fracture in the coal body during the ordinary hydraulic fracturing, local stress concentration, and pressure relief blind zone after fracturing.

This joint mode not only solves the problems that the direction of hydraulic fracturing crack is not easy to control, but also the crack propagation in the fracturing area is uneven. It is easy to form a high stress concentration area, and there is a "blind zone" of fracturing, but also increases the scope of impact of fracturing, which saves a lot of drilling engineering compared with ordinary drilling holes and improves the efficiency of pressure relief and antiextrusion. At the same time, the problems of uneven pressure relief and stress concentration in individual areas are supplemented by fixed-point hydraulic cutting to achieve uniform and efficient antipenetration purposes. A schematic diagram of the first cut and then press joint is shown in Figure 1.

3. Ultra-High Pressure Hydraulics First Press and Then Cut and Increase the Principle of Penetration

Hydraulics first press and then cut joint mode, that is, hydraulic fracturing is used to supplement the fracture within the influence range of hydraulic fracturing. The gap fracture is formed in the blank zone of the hydraulic fracturing affected area, and the fracture formed by hydraulic fracturing is conducted, and more fractures are formed. Through hydraulic fracturing operations to rapidly improve the permeability of the coal seam in the area and the gas extraction effect, after the completion of the hydraulic fracturing construction, the fracturing crack is uncontrollable. Although the cracks in the coal seam are generated in a large range, the permeability of the coal seam increases, and the coal body plays a decompression and permeability effect within the scope of the crack. However, the inhomogeneity of the physical and mechanical properties of the coal leads to the uncontrollable weak surface in the coal seam, resulting in uncontrollable hydraulic fracturing cracks. There is a blank zone affected by hydraulic fracturing within the scope of influence of the hydraulic fracturing, and the area with poor pressure relief effect is used as a "blind spot" of hydraulic fracturing, and there is a stress concentration in the uncontrolled area of the crack. The use of hydraulic cutting joints to accurately increase penetration and strengthen extraction, under the action of ground stress, and the fracturing cracks are connected with the fractured area of the joints, forming an overall pressure relief area, reducing the stress concentration, and effectively improving the gas permeability of the coal seam. This mode effectively combines the advantages of fracturing and fracture, solves the problem of stress concentration and uneven fracturing in the fracturing area, and realizes the accuracy of antiprotrusion. The precise antiprotrusion mode of pressing first and cutting is shown in Figure 2.

4. Ultra-High Pressure Hydraulics First Press and Then Cut and Increase the Principle of Penetration

Under the action of ultra-high pressure hydraulic force, when the coal body around the borehole exceeds its own strength, the hole wall is the plastic softening zone and the elastic zone are from inside to outside. The drilling mechanical model is shown in Figure 3. The model assumes the following:

① The borehole is subject to the stress P_0 of the original rock, and the side pressure coefficient $\lambda = 1$ is treated according to the axial symmetry problem, which is simplified to planar strain

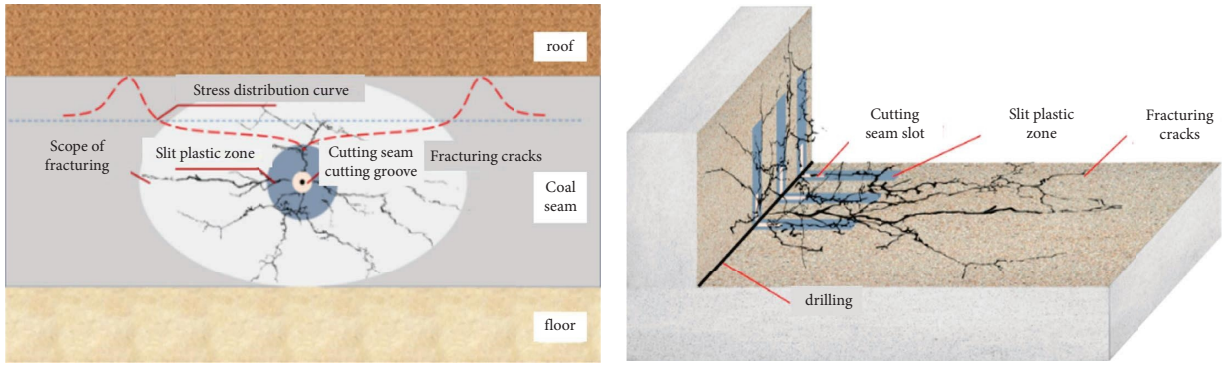

Figure 1: Schematic diagram of high efficiency anti-penetration mode of cutting before pressing. (a) Schematic diagram of fracture propagation profile after cutting. (b) Schematic diagram of the distribution plane of the slit after cutting.

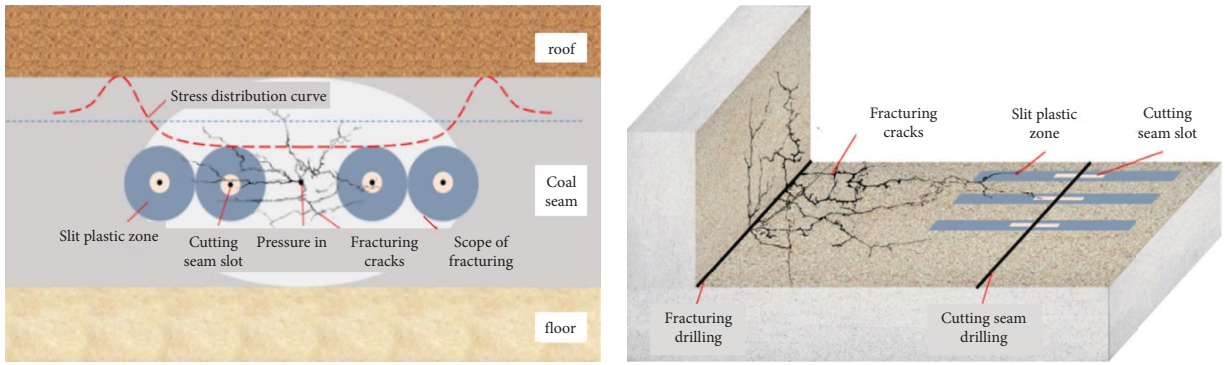

Figure 2: Schematic diagram of high efficiency anti-spike mode of pressing before cutting. (a) Schematic diagram of fracture propagation profile after compression. (b) Schematic diagram of the distribution plane of the crack before pressing and cutting.

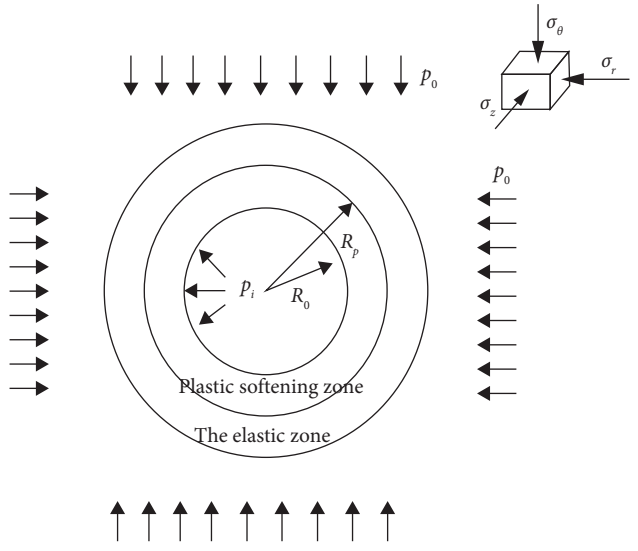

Figure 3: Borehole mechanical model.

② The coal around the borehole is homogeneous and isotropic, and the influence of borehole pressure relief on the borehole is not considered

③ R_0 is the drilling radius; σ_p is the peak intensity; σ_c is the residual strength; the hydraulic fracturing pressure p_i acts evenly on the wall of the drilled hole

Assuming that the compressive stress is positive and the tensile stress is negative, the deep borehole is subjected to ground stress, at this time:$\sigma_1 = \sigma_\theta$, $\sigma_3 = \sigma_r$, and $\sigma_2 = \sigma_z = \mu(\sigma_\theta + \sigma_r)$. The strength characteristics of the elastoplastic state of the borehole wall are described by the unified strength theory, and the expression is as follows:

$$\sigma_\theta = A_j \sigma_r + B_j, \tag{1}$$

$$\left.\begin{aligned} A_j &= \frac{(1+b\mu)\left(1+\sin\phi_j\right)}{\left(1-\sin\phi_j\right)(1+b) - b\mu\left(1+\sin\phi_j\right)} \\ B_j &= \frac{2(1+b)c_j\cos\phi_j}{\left(1-\sin\phi_j\right)(1+b) - b\mu\left(1+\sin\phi_j\right)} \end{aligned}\right\}, \tag{2}$$

where σ_θ, σ_r are the tangential stress and radial stress of the borehole wall, respectively. Since A_j, B_j are characterizing the parameters of the coal body, representing the relationship between the maximum principal stress and the minimum principal stress. The μ is for Poisson's ratio; j is the symbolic parameter; $j = e$ represents the initial internal friction angle φ_e and cohesion force c_e of the coal body; $j = p$ represents the friction angle φ_p and cohesion c_p of the plastic softening region; b is the median principal stress coefficient, $0 \le b \le 1$.

In the stress-strain curve, failure occurs when the strength of the coal body exceeds its ultimate strength, and this paper assumes that the residual friction angle φ_c and the residual cohesion c_c are unchanged. Plastic softening occurs when the strength of the coal body exceeds its peak strength, and the values of the friction angle φ_p and cohesion c_p in the plastic region gradually decrease with the increase in plastic strain, assuming that φ_p and c_p are linearly softened with the initial internal friction angle φ_e and cohesion force c_e. The softening coefficients k_φ and k_c are introduced, which are as follows:

$$\phi_p = \begin{cases} \phi_e, & \left(r \ge R_p\right), \\ k_\phi \phi_e, & \left(r \le R_p \text{and} \dfrac{\phi_s}{\phi_e} \le k \le 1\right), \end{cases}$$

$$c_p = \begin{cases} c_e, & \left(r \le R_p\right), \\ k_c c_e, & \left(r \le R_p \text{and} \dfrac{c_s}{c_e} \le k_c \le 1\right), \end{cases} \tag{3}$$

where k_φ, k_c are the internal friction angle and the cohesive softening coefficient. φ_e, φ_p, and φ_s are the initial internal friction angle, the friction angle of the plastic softening zone, and the residual internal friction angle of the coal body, respectively. c_e, c_p,c_s are the initial cohesion of the coal body, the cohesion, and residual cohesion in the plastic softening area, MPa. R_p is the radius of the plastic zone, m.

The drilled coal body is in the linear elastic state, p_y is set as the radial stress at the junction of the elastic zone of the coal body and the plastic softening zone, and the elastic zone of the coal body is regarded as a thick-walled cylinder under the joint action of p_y and ground stress p_0. It can be seen that the elastic zone stress is as follows:

$$\begin{cases} \sigma_{re} = p_y \dfrac{R_p^{\,2}}{r^2} + p_0\left(1 - \dfrac{R_p^{\,2}}{r^2}\right), \\ \sigma_{\theta e} = -p_y \dfrac{R_p^{\,2}}{r^2} + p_0\left(1 + \dfrac{R_p^{\,2}}{r^2}\right), \end{cases} \tag{4}$$

where σ_{re} is radial stress in the elastic zone, MPa. $\sigma_{\theta e}$ is the tangential stress of the elastic region, MPa. r is the distance from any point in the coal body to the center of the circle, m. p_0 is the ground stress, MPa. p_y is the stress at the elastoplastic junction, MPa.

At the elastoplastic junction $r = R_p$, formula (5) satisfies formula (1) and the radial stress is continuous, and the finishing can be obtained as follows:

$$p_y = \frac{2p_0 - B_e}{1 + A_e}. \tag{5}$$

Any of the study unit points in the coal body satisfy the equilibrium differential equation:

$$\frac{\mathrm{d}\sigma_r}{\mathrm{d}r} + \frac{\sigma_r - \sigma_\theta}{r} = 0. \tag{6}$$

Substituting equation (1) into equation (6) and integrating, take $\sigma_r | r = R_0 = p_i$ as the boundary condition, the radial and tangential stresses of the plastic region can be obtained as follows:

$$\begin{cases} \sigma_{rp} = S_1 + \left(p_i - S_1\right)\left(\dfrac{R_0}{r}\right)^{1-A_p}, \\ \sigma_{\theta p} = S_1 + A_p\left(p_i - S_1\right)\left(\dfrac{R_0}{r}\right)^{1-A_p}. \\ S_1 = \dfrac{B_p}{1 - A_p}. \end{cases} \tag{7}$$

The radial stress σ_r is continuous at the elastoplastic junction, which is $\sigma_{rp} | r = R_\mathrm{p} = \sigma_{re} | r = R_\mathrm{p}$.The radius of the plasticity zone of the first type (7) and the first type of (4) of the first type of plasticity zone is as follows:

$$R_p = R_0 \cdot \left[\frac{p_y - S_1}{p_i - S_1}\right]^{1/1-A_p}. \tag{8}$$

5. Numerical Simulation Analysis of Ultra-High Pressure Hydraulics Combined with Permeation PFC

Under the action of ultra-high pressure hydraulic force, when the coal body around the borehole exceeds its own strength, the hole wall is the plastic softening zone and the elastic zone from the inside to the outside. The drilling mechanical model is shown in Figure 3. The model assumes the following:

The particle flow discrete element method (PFC) is based on the mechanics of discontinuous media to study the germination, expansion, and penetration of fractures, which can truly express the geometric characteristics of jointed rock masses, facilitate the handling of nonlinear deformation and destruction, and reflect the different physical relationships between multiphase media through a variety of connection methods between cells, which can effectively study noncontinuous phenomena such as cracking and separation. There are countless mesoscopic cracks in coal rocks, especially soft coal bodies, showing obvious inelastic deformation characteristics, and these mesoscopic cracks develop into macroscopic cracks or until they break down under increased loads. In the particle flow discrete element, when the contact point node is destroyed, the corresponding particles will produce cracks, and new cracks will be generated at the initial crack tip as a sign of hydraulic fracturing. The nonlinear deformation failure process of the fracture can be analyzed by direct and indirect methods. The indirect method uses the constitutive relationship to analyze the failure process, generally assumes the fractured coal body as an ideal uniform material, reflects the weakening of the overall strength of the fractured coal body through a certain constitutive relationship, and expresses the microstructure failure process in the coal body in this way. The direct method is a mesoscopic simulation method, which assumes that the fracture coal material is a collection of various microstructures, or some particle combinations connected at the contact point. The failure process of the fractured coal body can be directly simulated by the microstructure and particle rupture, and the fractured coal body can be studied mescologically without simulation through complex constitutive models.

The PFC numerical calculation software is a kind of software based on particle flow theory, which links the microstructure of materials with macroscopic mechanical reactions, and directly simulates material failure from a mesoscopic perspective, which is suitable for materials that are difficult to accurately describe their properties through constitutive relationships based on uniform media, such as fractured rock masses. The bonding parameters of the particles determine the location and number of initial microcracks, so microcracks can only be formed in the connection contact model. The position and size of the two particles determine the location and geometry of the cracks, which can be simplified to a cylindrical surface represented by the center point position, normal direction, thickness, and radius parameters.

5.1. First Cut and Then Press Combined with Unloading Coal Seam Fracture and Stress Distribution. The model adopts a two-dimensional plane model. The direction length is 200 m, the height is 200 m, the drilling diameter is 113 mm, the cutting pressure is 100 MPa, the test site elevation is about 550 m, the vertical stress reaches 17.7 MPa, the pressure measurement coefficient is 1, and the horizontal stress is 17.7 MPa. The model schematic diagram is shown in Figure 4.

First, hydraulic cutting is used to form a slot, and a pressure of 25 MPa is applied to the periphery of the groove for fracturing, and the distribution of fracture, main stress, and permeability of the coal seam after fracturing is analyzed. The fissure distribution of coal seam in the process of drilling construction, hydraulic cutting, and hydraulic fracturing is shown in Figures 5–7, respectively, and the maximum main stress distribution curve on the midline of the test borehole level is monitored in the simulation.

Figure 5 shows the distribution of coal cracks after drilling construction. It can be seen from the figure that the fissures in the coal body around the drilling hole are not obvious after the construction of the borehole, and basically maintain the original state. The stress of the coal body around the borehole is evenly distributed and is basically in a state of stress equilibrium. Only the drilling is excavated, creating plastic deformation zones and elastic zones around the borehole, resulting in reduced seam stress. Figure 6 shows the distribution of coal cracks after drilling and cutting. It can be seen that after drilling and cutting, a circular gap is formed around the drilling hole, and the coal body around the gap groove is damaged or plastically deformed, forming a crack. The stress of the coal body around the trough is concentrated and transferred to the deep part of the coal body, and a stress-reduced pressure relief zone is formed around the slot area. Figure 7 shows the distribution of fractures in coal with a fracturing pressure of 25 MPa, as the water injection pressure increases, when the fissure expands to a certain extent. The expansion rate begins to slow down, and the secondary fissures are gradually interconnected to form a highly complex fracture network, but with the continuous development of the fissures in the coal seam, the degree of stress concentration is becoming more and more serious.

In the affected area of fracturing, the fractures are mainly elliptical in distribution. In terms of the degree of damage of the coal body, the coal body in the area near the fracturing hole is better than the coal body far from the fracturing hole area. From the change of water injection pressure during the fracturing process, it can be seen that the cracking pressure is about 13 MPa, and the radius of influence of hydraulic fracturing can reach 45–55 m.

After hydraulic fracturing of the coal seam, the original stress balance state of the coal seam is destroyed, resulting in a decrease in the stress value of the coal seam in the area near the fracturing hole, forming a pressure relief zone. However, the stress value of the coal seam around the pressure discharge zone increases, forming a stress concentration area. Therefore, according to the stress distribution of the coal seam after fracturing, the coal seam around the fracturing

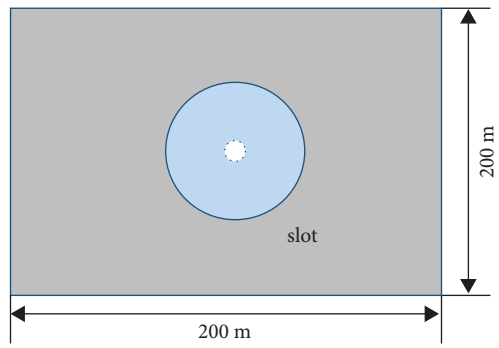

Figure 4: Joint numerical model of coal seam cutting pressure.

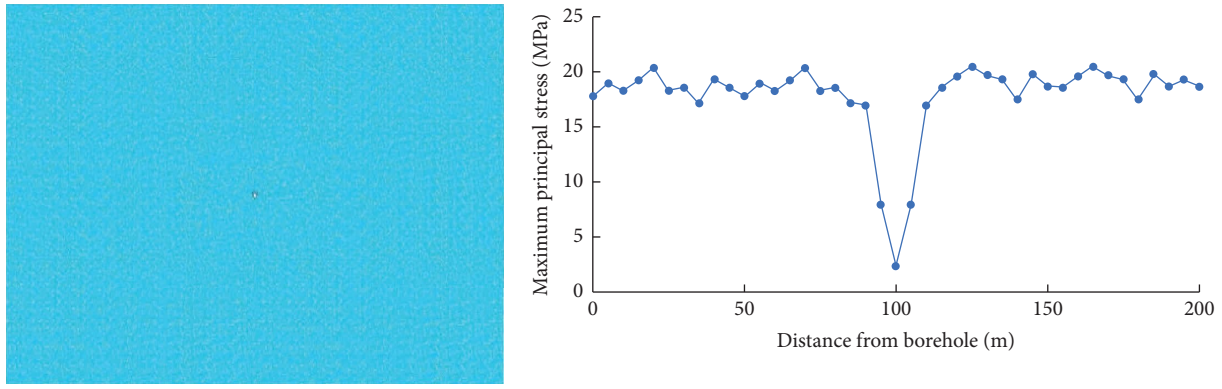

Figure 5: Fracture and stress distribution of coal seam after drilling. (a) Distribution of fractures. (b) Stress distribution condition.

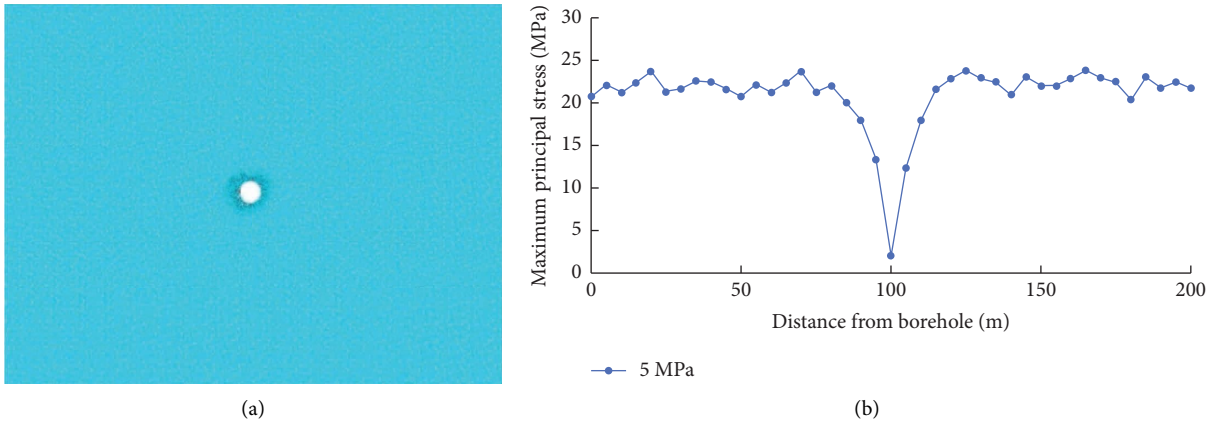

Figure 6: Fracture and stress distribution of borehole after slit. (a) Distribution of fractures. (b) Stress distribution condition.

hole can be divided into stress reduction zone (pressure relief area), stress concentration area, stress transition area, and original stress area from near and far.

5.2. First Press and Then Cut Combined with Unloading Coal Seam Fracture and Stress Distribution. The model adopts a two-dimensional plane model, the direction length is 200 m, the height is 200 m, and the drilling diameter is 113 mm, which is consistent with the model of Figure 4, as shown in Figure 8. The central fracturing hole is located in the center of the coal seam and is set to 113 mm in diameter. The test site elevation is about 550 m, the vertical stress reaches 17.7 MPa, the side pressure coefficient is 1, and the horizontal stress is 17.7 MPa. 25 MPa pressure is applied to the periphery of the borehole for fracturing, and after the completion of the fracturing, hydraulic fracture drilling is

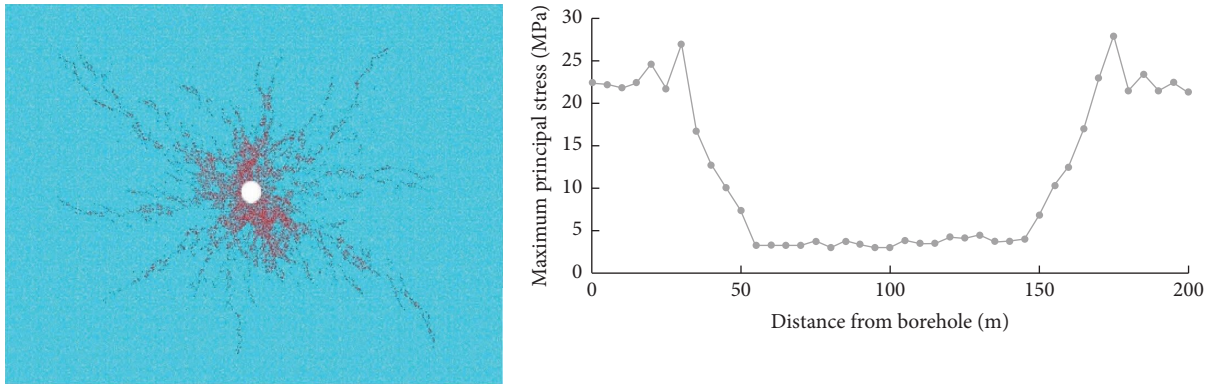

(a) (b)

Figure 7: Fracture and stress distribution when fracturing pressure is 25 MPa. (a) Distribution of fractures. (b) Stress distribution condition.

carried out in the blank area of the fracture according to the fracture and stress distribution. The distribution of fracture, main stress, and permeability of the coal seam after fracturing and cutting is analyzed.

Figures 9–11 are the fissure distribution of the coal seam and the maximum main stress distribution curve on the midline of the drilling level of the ordinary borehole hydraulic fracturing process, respectively.

Figure 9 shows the distribution of coal cracks after drilling construction. It can be seen from the figure that after the construction of the borehole, the fracture of the coal body around the borehole is not obvious and basically maintains the original state. The stress of the coal body around the borehole is evenly distributed and is basically in a state of stress equilibrium. Only due to the excavation of the drilled hole, the plastic deformation zone and the elastic zone are generated around the drilled hole, resulting in a reduction in the stress of the coal seam.

Figure 10 shows the fracture distribution of coal with a fracturing pressure of 25 MPa. As can be seen from the figure, when the fissure expands to a certain extent, the number of new fissures decreases, and there is a stress-concentrated area. In the affected area of fracturing, the distribution of fracture fractures is mainly in the direction of main stress, and the other regions have less fracture development and there are blank areas. The fracture development is uneven. After the use of hydraulic cuts, the number of cracks increases, and the stress concentration area caused by hydraulic fracturing is significantly relieved. From the change of water injection pressure during the fracturing process, it can be seen that the cracking pressure is about 16 MPa, and the influence radius of hydraulic fracturing can reach 35~45 m.

Figure 11 shows the fracture distribution and stress distribution after hydraulic fracture in the nonformation area of the coal seam after the fracturing pressure is 25 MPa. As can be seen from the figure, after the hydraulic fracture is carried out in the later stage, the fracture blank zone within the influence range of the original hydraulic fracturing generates a crack. The fracture that has been generated can be further increased. The stress concentration area is redistributed to play a role in depressurization.

Compared with the same model, there is a big difference between the cutting sequence of ultra-high pressure water jet and the fracture and horizontal direction of the discharge coal seam:

(1) The cracking pressure of the coal seam with the combined pressure of cutting first and then pressing is 13 MPa, and the radius of influence of hydraulic fracturing can reach 45–55 m. The cracking pressure of the coal seam of first pressure and then cutting and unloading coal seam is 16 MPa, and the radius of influence of hydraulic fracturing can reach 35–45 m.

(2) The first cut and then the combined pressure discharge coal seam destroys the original stress balance state of the coal seam, causing the stress value of the coal seam in the area near the fracturing hole to decrease, forming a pressure relief area. The stress distribution is more uniform, at a low value, forming a better pressure relief area, and the stress value of the coal seam around the pressure relief area is increased, forming a stress concentration area. In the area affected by fracturing, the distribution of fracture fractures is mainly along the direction of main stress. The fracture development in other areas is less, and there are blank areas. The development of fractures is uneven, after the use of hydraulic fractures, the number of fractures increases, and the stress concentration area caused by hydraulic fracturing is obvious. But there are pressure fluctuations and instability in the pressure relief area.

In summary, after the cutting pressure combination, the pressure relief of the coal body can be uniform and sufficient. The overall gas permeability coefficient of the coal body can be greatly improved. The scope of influence of extraction can be increased, and the extraction effect can be significantly improved. At the same time, the stress after the coal body is cut and the cracking pressure during hydraulic fracturing is reduced.

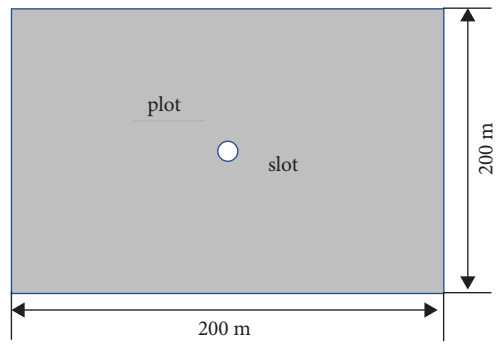

Figure 8: Numerical model for hydraulic fracturing of coal seam.

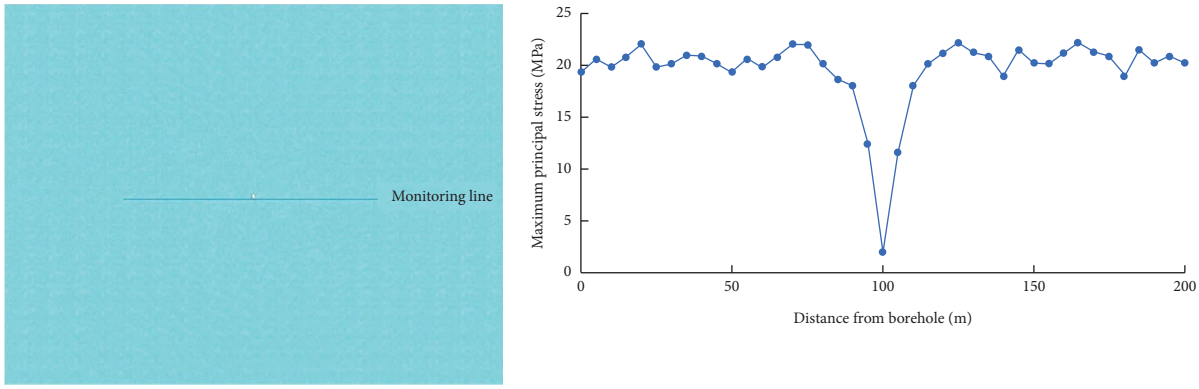

(a) (b)

Figure 9: Fracture and stress distribution of coal seam after drilling. (a) Distribution of fractures. (b) Stress distribution condition.

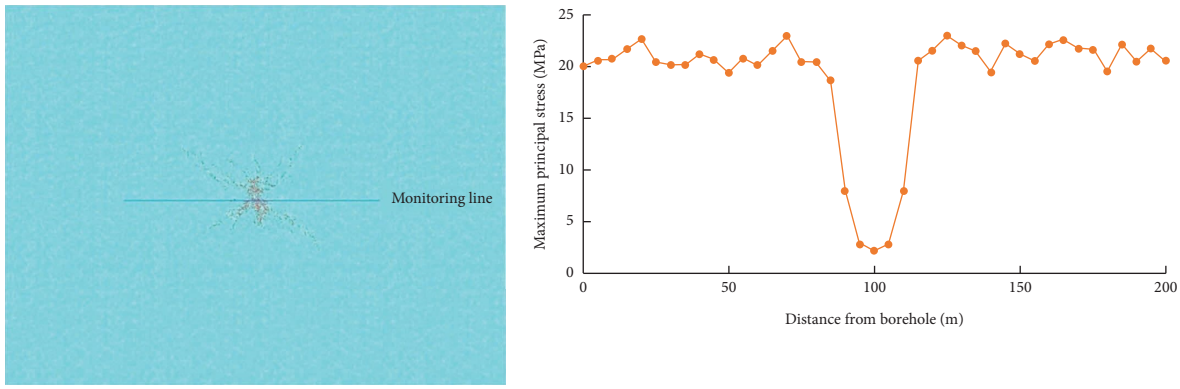

(a) (b)

Figure 10: Fracture and stress distribution of 25 MPa pressure fractured coal seam. (a) Distribution of fractures. (b) Stress distribution condition.

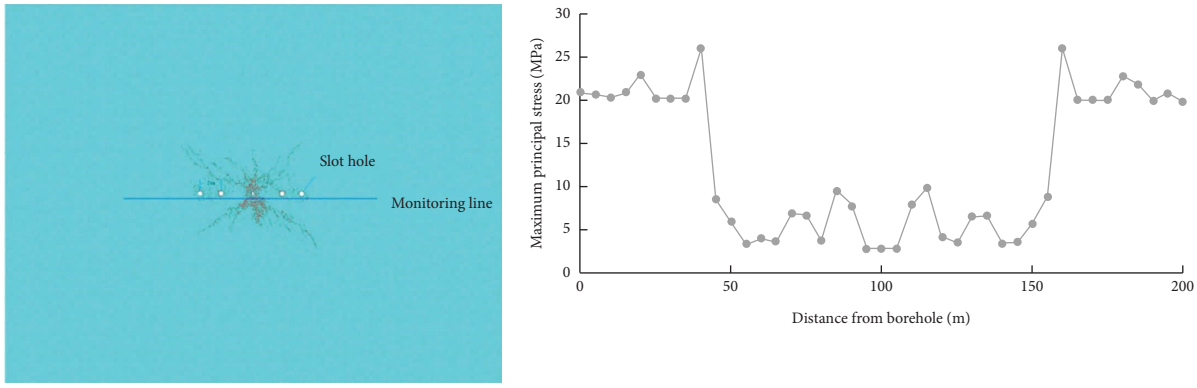

(a) (b)

Figure 11: Fracture and stress distribution of seam after hydraulic fracturing. (a) Distribution of fractures. (b) Stress distribution condition.

6. Engineering Application of Ultra-High Pressure Hydraulic Cutting Combined Process Technology

6.1. Application of Combined Pressure Relief and Antireflection after Cutting through Layer Drilling

6.1.1. Project Summary. 220106 working surface is located in the 2201 mining area, the maximum gas content of 1 coal seam is 6.8 m^3/t, and the gas pressure is 1.22 MPa. The first coal seam group includes 1 coal and 1 upper coal. The average upper coal is 3.9 m, the average upper coal is 2.8 m, and the average gangue lost between 1 coal and 1 upper coal is 1.0 m. The inclination angle of the coal seam is 2°–12°, and the average is 6°. The working surface is directly topped with sandy mudstone with an average thickness of 6.7 m, and the old top is quartz sandstone with an average thickness of 17.8 m. The application site elevation is about 523.0−−559.6 m, a total of 7 cut pressure combined drilling holes are constructed, and the floor plan is shown in Figure 12.

6.1.2. Application of Cutting Pressure Combined with Anti-reflection Technology

(1) Cut-Pressure Combined Drilling Implementation. The length of the seven cutting pressure combined drilling coal hole sections is 11–16 m. The maximum pressure during the cutting period is 90–100 MPa. The cutting gap is 3 m, and the single knife cutting time is 5–10 min. During the cutting operation, the drilling and rebating water and slag return is smooth. The coal output of a single knife is 0.34–0.56 t. The average single knife output is about 0.43 t, and the equivalent radius of the average cut is 2.54 m.

After the completion of drilling and cutting, the hole is sealed immediately. The hydraulic fracturing is carried out after 48 h. The maximum pressure of fracturing is 22–27 MPa. The number of fractures per drilling hole is 3 times. The fracturing time is 19–28 h, and the total amount of water injection per borehole is 109.6–132.4 m^3.

(2) Drilling Quantity Analysis. The spacing between the layout of the extraction drilling holes in the application area is 13 m × 13 m, and a total of 183 extraction drilling holes are constructed, with a drilling volume of about 11800 m. Compared with the conventional drilling arrangement of the mine (the layout spacing is 10 m × 10 m, and 297 extraction drilling holes need to be constructed, about 19200 m), the drilling volume can be saved by about 38%.

(3) Pumping Volume Analysis, Pumping Pure Volume. The concentration and extraction scalculus of the drilling hole in the application area are shown in Figures 13 and 14.

It can be seen from the figure that the extraction concentration in the combined cutting pressure area is 10% to 40%. The concentration fluctuation is relatively stable. The attenuation is small. The extraction purity is 5.12–10.13 m^3/min, and the average single-hole extraction purity is 0.0245 m^3/min, which is 2.3 times that of the ordinary drilling single-hole extraction purity of 0.0108 m^3/min.

(4) Extraction Standard Time. According to the drilling and extraction situation in the application area, when the extraction drilling hole extraction is 47 days, the extraction rate reaches 30%. A total of 14 residual gas content were tested, and the test result was 3.98–4.75 m^3/t. The extraction standard was achieved. The extraction time is 41% lower than the 80 days of ordinary drilling and extraction.

6.2. Application of Combined Pressure Relief and Anti-Reflection Improvement through Layer Drilling

6.2.1. Project Summary. The application site of the drilling is 220106, the working surface is located in the outer section of the 2201 mining area (the strike length is about 170 m, and the strike width is about 190 m), a total of 3 fracturing

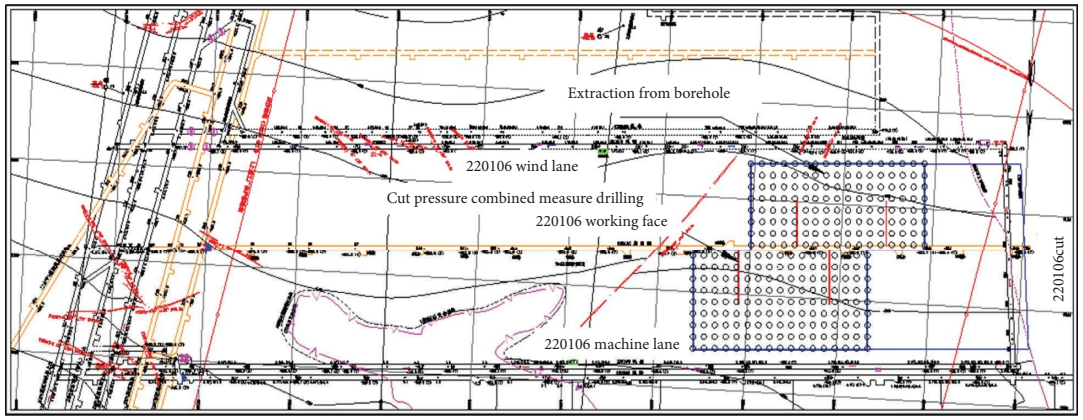

Figure 12: Cut pressure combined measures plan.

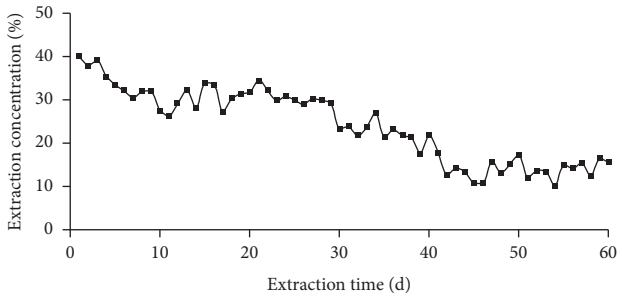

Figure 13: Change curve of extraction concentration.

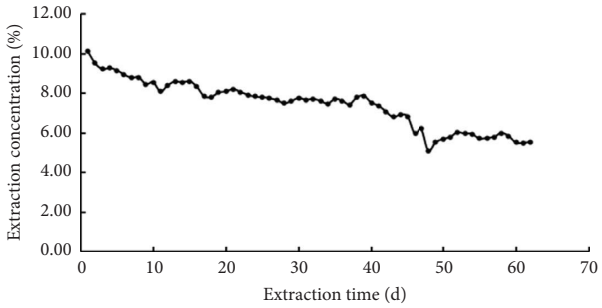

Figure 14: The net volume change curve of extraction.

drilling holes are constructed, and the spacing is cut according to the 26 m × 26 m spacing, and the floor plan is shown in Figure 15.

6.2.2. Application of Compression Cutting Combined with Antireflection Technology

(1) Cut-Pressure Combined Drilling Implementation. The maximum pressure of fracturing is 22–27 MPa, and the number of fracturing times for each borehole is 3 times. The fracturing time is 21–32 h, and the total water injection of each borehole is 117.8–145.2 m^3.

After the completion of fracturing, the drilling hole is drilled according to the construction of 13 m × 13 m spacing in the control area, and the hydraulic cutting measures are constructed according to the 20 m × 20 m spacing. The maximum pressure during the cutting period is 90–100 MPa. The cutout spacing is 3 m, and the single knife cutting time is 5–10 min. A total of 91 cut holes were implemented, and the drilling reflow water and slag return was smooth during the seam operation. The coal output of a single knife was 0.31–0.62 t. The average single knife coal output was about 0.41 *t*, and the equivalent radius of the average cut was 2.52 m.

(2) Drilling Quantity Analysis. The spacing between the layout of the extraction drilling holes in the application area is 13 m × 13 m, and a total of 183 extraction drilling holes are constructed, with a drilling volume of about 11800 m. Compared with the conventional drilling arrangement of the mine (the layout spacing is 10 m × 10 m, and 297 extraction drilling holes need to be constructed, about 19200 m), the drilling volume can be saved by about 38%.

(3) Pumping Volume Analysis, Pumping Pure Volume. The concentration and extraction scalarity of drilling in the application area are shown in Figures 16 and 17. It can be seen from the figure that the extraction concentration in the combined cutting pressure area is 30% to 40%. The concentration fluctuation is relatively stable. The attenuation is small. The extraction purity is 3.6–6.8 m^3/min, and the average single-hole extraction purity is 0.026 m^3/min, which is 2.4 times that of the ordinary drilling single-hole extraction purity of 0.0108 m^3/min.

(4) Extraction Standard Time. According to the drilling and extraction situation in the application area, when the extraction drilling hole extraction is 43 d, the extraction rate reaches 30%. A total of 5 residual gas content were tested, and the test result was 3.76–4.52 m^3/t, and the extraction standard was achieved. The extraction time is 35% less than the ordinary drilling and extraction time of 66 d.

6.3. Economic Benefits

6.3.1. Direct Economic Benefit Analysis. After the 220106 working surface adopts the measures of cutting pressure

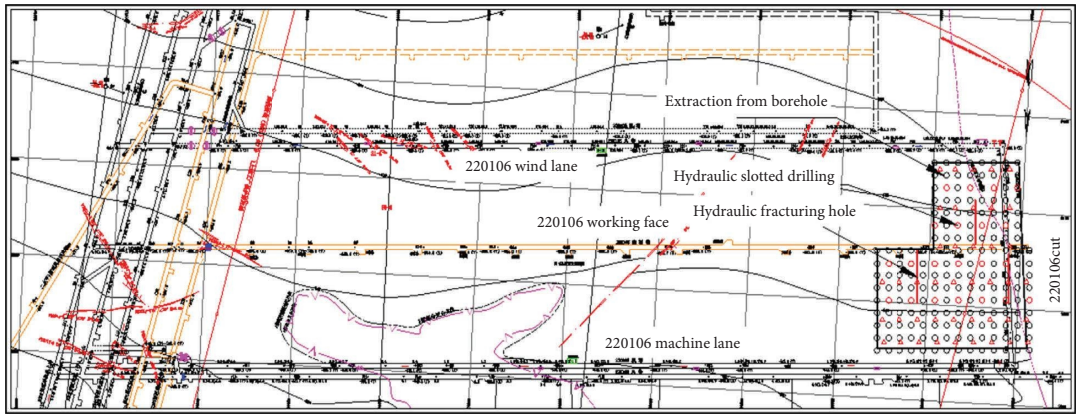

Figure 15: Pressure before cutting combined measures floor plan.

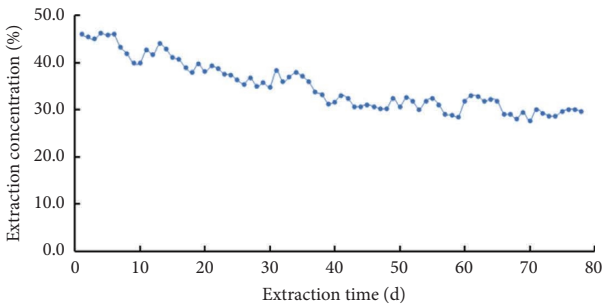

Figure 16: Change curve of extraction concentration.

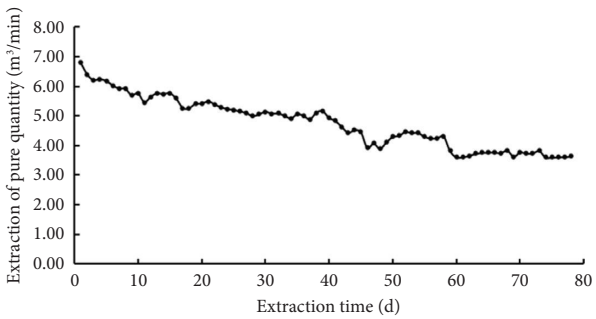

Figure 17: The net volume change curve of extraction.

combined pressure relief and removal. The amount of drilling engineering by 34000 m and the amount of drilling by 10000 m is reduced by 10000 m. It can reduce the maintenance of 33 d of drilling holes in the 220106 working surface (length 860 m) and 36 d of maintenance of the bottom plate lane (900 m long) extraction drilling, calculated at 30 yuan/m·d.

Save engineering costs: (34000 + 10000) m × 300 yuan/m = 13.2 million yuan

Saving maintenance investment: 860 m × 2 × 30 yuan/m·d × 33 d + 900 m × 30 yuan/m·d × 36 d = 2.6748 million yuan

In summary, a total of 15.8748 million yuan of direct economic benefits have been generated.

6.3.2. Indirect Economic Benefit Analysis. 220106 working surface drilling and extraction time are shortened by 33 and 25 d. The working surface is returned to the production in advance, and the early recovery of the working surface produces indirect economic benefits:

$$25 \times 6000\ \text{t/d} \times 600\ \text{yuan/t} = 90\ \text{million yuan}$$

Xinji No.2 mine generated a total of 90 million yuan in indirect economic benefits.

7. Conclusions

(1) The coal seam initiation pressure of ultra-high pressure water jet cutting pressure combined with pressure relief is 13 MPa, and the influence radius of hydraulic fracturing is 45–55 m. The initiation pressure of coal seam is 16 MPa, and the influence radius of hydraulic fracturing is 35–45 m. The combined technology of cutting pressure can make the pressure relief of coal body uniform and sufficient, the overall permeability coefficient of coal body is greatly improved, the influence area of extraction is enlarged, and the extraction effect is significantly improved. At the same time, the stress after the coal seam cutting is reduced, and the fracturing pressure during hydraulic fracturing is reduced.

(2) After hydraulic slit, the initiation pressure of coal seam decreases, and the influence radius of hydraulic fracturing increases, with an influence range of 46–56 m. The permeability within the influence area increases by 25 to 30 times. The permeability coefficient of coal seam is 0.775 $m^2/MPa^2 \cdot d$ after the process of cutting pressure combined with pressure relief and permeability improvement, which is 23 times of the original coal body. The gas permeability of coal seam is increased significantly by hydraulic cutting first and then fracturing.

(3) The extraction concentration in the combined area of drilling and cutting pressure is 10%–40%, and the concentration fluctuation is relatively stable and the attenuation is small. The extraction purity is

5.12–10.13 m^3/min, and the average single hole extraction purity is 0.0245 m^3/min, which is 2.3 times of the single hole extraction purity of ordinary drilling. The time to reach the standard of extraction is 32.8 d shorter than that of ordinary drilling. The extraction concentration in the combined area of borehole and pressure cutting is 30%–40%, the concentration fluctuation is relatively stable and the attenuation is small. The extraction pure volume is 3.6–6.8 m^3/min, and the average single hole extraction pure volume is 0.026 m^3/min, which is 2.4 times of the single hole extraction pure volume is 0.0108 m^3/min of ordinary drilling. The time to reach the standard of extraction is 25 d shorter than that of ordinary drilling.

(4) The pressure cutting combined with pressure relief and antireflection technology has been successfully applied in Xinji coal mine, and has created good economic benefits. This technology has a wide application prospect.

Data Availability

The data presented in this study are available upon request from the corresponding author.

Conflicts of Interest

The authors declare that they have no conflicts of interest.

Acknowledgments

This work was supported by the Open Project of Building Structure and Underground Engineering Key Laboratory of Anhui Province (grant no. KLBSUE-2022-03).

References

[1] D. Y. Hao, Q. S. Bai, W. L. Li, and Z. Q. Yang, "Mining technology of "mining, dressing and filling + pumping" with less gangue in deep high gas mine protection layer," *Journal of Mining & Safety Engineering*, vol. 37, no. 1, pp. 93–100, 2020.

[2] W. P. Xiang, P. H. Zhang, Z. C. Li et al., "Discussion on abnormal geological characteristics and development technology of deep coalbed methane," *Coal Engineering*, vol. 54, no. 6, pp. 158–164, 2022.

[3] Y. P. Cheng, H. Y. Liu, P. K. Guo, R. K. Pan, and L. Wang, "Permeability evolution and unloading antireflection theoretical model of deep gas-bearing coal body," *Journal of China Coal Society*, vol. 39, no. 8, pp. 1650–1658, 2014.

[4] Y. Ding, Y. Wei, Z. C. Wang, L. Qin, P. X. Zhao, and H. F. Lin, "Numerical simulation and application of hydraulic slit relief and reflection improvement in coal seam drilling through layers," *Mining Research and Development*, vol. 42, no. 8, pp. 182–188, 2022.

[5] F. F. Liu, Y. Y. Huang, Q. Xu et al., "Effect of high pressure water jet slotting on pressure relief and reflection improvement of coal seam," *Safety In Coal Mines*, vol. 45, no. 9, pp. 165–168, 2014.

[6] Y. Liu, A. He, M. J. Wei, and H. Z. Wen, "Inducement and new method of water jet pressure relief and permeability improvement for hole plugging," *Journal of China Coal Society*, vol. 41, no. 8, pp. 1963–1967, 2016.

[7] H. Li, M. B. Shi, and Y. Li, "Research on anti-outburst technology of strong outburst and soft close distance coal seam Group in Shimen," *Journal of Safety Science and Technology*, vol. 10, no. 1, pp. 98–102, 2014.

[8] Z. X. Xu, "Combined anti-reflection technology of ultra-high pressure hydraulic slit and hydraulic fracturing in low permeability coal seam," *Coal Science and Technology*, vol. 48, no. 7, pp. 311–317, 2020.

[9] K. S. Zhao, J. Y. Li, T. H. Chai et al., "Optimization of pre-slit inclination Angle and anti-punching practice in directional hydraulic fracturing of thick and hard sandstone roof in Shaan-Mongolia area," *Journal of China Coal Society*, vol. 45, no. S1, pp. 150–160, 2020.

[10] L. W. Cao, J. Nian, and B. X. Lv, "Study on comprehensive anti-reflection technology of hydraulic slit (fracturing)," *Coal Technology*, vol. 36, no. 7, pp. 199–201, 2017.

[11] K. Zhong, Z. W. Chen, S. W. Zhao, K. C. Qin, X. H. Cao, and D. H. Xie, "Monitoring and evaluation of anti-flood effect of hydraulic fracturing of hard roof in coal mine," *Journal of Central South University*, vol. 53, no. 7, pp. 2582–2593, 2022.

[12] H. X. Shi, P. L. Zhao, T. J. Li, J. R. Wang, and F. C. Wu, "Anti-reflection technology of hydraulic fracturing for low permeability and high gas coal seam in complex structural belt," *Mining Safety & Environmental Protection*, vol. 49, no. 3, pp. 101–106, 2022.

[13] G. Q. Li, Z. Y. Deng, T. Q. Hu et al., "Mesoscopic law of hydraulic fracturing stress and fracture evolution in coal seam," *Coal Geology & Exploration*, vol. 50, no. 6, pp. 30–40, 2022.

[14] J. Y. Zhang, F. Z. Huang, and F. Ji, "Coal, rock and gas dynamic disaster prevention and control technology based on hydraulic slit pressure relief," *Coal Science and Technology*, vol. 49, no. 1, pp. 133–141, 2021.

[15] Z. S. Li and J. Z. Lu, "Application of ultra-high pressure hydraulic slotting technology in bedding drilling to strengthen gas extraction," *Coal Technology*, vol. 39, no. 2, pp. 121–124, 2020.

[16] X. B. Feng, M. C. Huang, and J. L. Zhang, "Application of high pressure hydraulic slit technology in coal seam gas drainage through floor," *Coal Engineering*, vol. 6, pp. 35–37, 2010.

[17] L. Z. Ge, D. X. Mei, J. Y. Jia, Y. Y. Lu, and W. B. Xia, "Study on the influence radius of high pressure water jet slotting drilling," *Journal of Mining & Safety Engineering*, vol. 31, no. 4, pp. 657–664, 2014.

[18] H. X. Li, Y. Y. Lu, Y. Zhao, Y. Kang, and P. D. Zhou, "Study on improving permeability of soft coal seam by high pressure pulse water jet," *Journal of China Coal Society*, vol. 33, no. 12, pp. 1386–1390, 2008.

[19] P. J. Tang, L. S. Yang, and P. L. Li, "Numerical simulation of the effect of different hydraulic slit arrangement on pressure relief and outburst prevention," *Chinese Journal of Geological Hazard and Control*, vol. 23, no. 1, pp. 61–66, 2012.

[20] Z. J. Jia, Q. J. Ge, H. W. Zhen, and D. Zhao, "Study on anti-reflection technology and application of hydraulic fracturing," *China Safety Science Journal*, vol. 30, no. 10, pp. 63–68, 2020.

[21] D. D. Chen, Q. S. Sun, J. Zhang, Z. J. Zhao, G. K. Zheng, and Y. B. Jia, "Anti-reflection technology system and engineering practice of directional long borehole hydraulic fracturing coal seam," *Coal Science and Technology*, vol. 48, no. 10, pp. 84–89, 2020.

[22] B. Q. Mou, "Enhanced anti-reflection technology of hydraulic fracturing of long borehole through borehole," *Journal of Safety Science and Technology*, vol. 13, no. 8, pp. 164–169, 2017.
[23] M. K. Hubbert and D. G. Willis, "Mechanics of hydraulic fracturing," *Transactions of the AIME*, vol. 210, no. 1, pp. 153–168, 1957.
[24] K. Y. Ma, G. Z. Liu, and J. Zhou, "Experimental study on the correlation between fracture wall failure behavior and water injection flow rate," *Journal of Safety Science and Technology*, vol. 12, no. 6, pp. 82–87, 2016.
[25] C. Y. Lv, "Application of hydraulic fracturing technology in mine with high gas and low permeability," *Journal of Chongqing University*, vol. 33, no. 7, pp. 102–107, 2010.
[26] M. J. Bouteca, "Hydraulic fracturing model based on a three-dimensional closed form: tests and analysis of fracture geometry and containment," *SPE Production Engineering*, vol. 3, no. 4, pp. 445–454, 1988.
[27] L. Z. Lian, J. Zhang, A. H. Wu, X. X. Wang, and B. Xue, "Fluid-structure coupling numerical simulation of hydraulic fracturing expansion," *Rock and Soil Mechanics*, vol. 11, no. 3, pp. 3021–3026, 2008.
[28] L. Bjerrum, J. K. T. L. Nash, R. M. Kennard, and R. E. Gibson, "Hydraulic fracturing in field permeability testing," *Géotechnique*, vol. 22, no. 2, pp. 319–332, 1972.
[29] D. Chen, N. Li, and W. C. Sun, "Rupture properties and safety assessment of raw coal specimen rupture process under true triaxial hydraulic fracturing based on the source parameters and magnitude," *Process Safety and Environmental Protection*, vol. 158, pp. 661–673, 2022.
[30] Z. G. Deng, B. S. Wang, and X. B. Huang, "Study on hydraulic fracture propagation behavior of coal rock," *Chinese Journal of Rock Mechanics and Engineering*, vol. 20, no. 3, pp. 3489–3493, 2004.
[31] S. M. Liu, X. L. Li, D. K. Wang, and D. M. Zhang, "Investigations on the mechanism of the microstructural evolution of different coal ranks under liquid nitrogen cold soaking," *Energy Sources*, pp. 1–17, 2020.
[32] X. M. Zhou, S. Wang, X. L. Li et al., "Research on theory and technology of floor heave control in semicoal rock roadway: taking longhu coal mine in Qitaihe mining area as an Example," *Lithosphere*, vol. 2022, no. 11, Article ID 3810988, 2022.
[33] S. Wang, X. L. Li, and Q. Z. Qin, "Study on surrounding rock control and support stability of Ultra-large height mining face," *Energies*, vol. 15, no. 18, 2022.
[34] X. L. Li, S. J. Chen, S. Wang, M. Zhao, and H. Liu, "Study on in situ stress distribution law of the deep mine taking Linyi Mining area as an example," *Advances in Materials Science and Engineering*, vol. 2021, no. 4, Article ID 5594181, 11 pages, 2021.
[35] H. Y. Liu, B. Y. Zhang, X. L. Li et al., "Research on roof damage mechanism and control technology of gob-side entry retaining under close distance gob," *Engineering Failure Analysis*, vol. 138, no. 5, Article ID 106331, 2022.
[36] S. Tang, J. Li, S. Ding, and L. Zhang, "The influence of water-stress loading sequences on the creep behavior of granite," *Bulletin of Engineering Geology and the Environment*, vol. 81, no. 11, 2022.
[37] X. Liang, S. Tang, C. Tang, L. Hu, and F. Chen, "Influence of water on the mechanical properties and failure behaviors of sandstone under triaxial compression," *Rock Mechanics and Rock Engineering*, vol. 56, 2023.
[38] Q. Yin, J. Wu, Z. Jiang et al., "Investigating the effect of water quenching cycles on mechanical behaviors for granites after conventional triaxial compression," *Geomechanics and Geophysics for Geo-Energy and Geo-Resources*, vol. 8, no. 2, 2022.
[39] Y. Wang, C. Zhu, M. He, X. Wang, and H. Le, "Macro-meso dynamic fracture behaviors of Xinjiang marble exposed to freeze thaw and frequent impact disturbance loads: a lab-scale testing," *Geomechanics and Geophysics for Geo-Energy and Geo-Resources*, vol. 8, no. 5, 2022.
[40] Q. Wang, B. Jiang, S. Xu et al., "Roof-cutting and energy-absorbing method for dynamic disaster control in deep coal mine," *International Journal of Rock Mechanics and Mining Sciences*, vol. 158, Article ID 105186, 2022.
[41] Q. Wang, S. Xu, Z. Xin, M. He, H. Wei, and B. Jiang, "Mechanical properties and field application of constant resistance energy-absorbing anchor cable," *Tunnelling and Underground Space Technology*, vol. 125, Article ID 104526, 2022.
[42] F. Xiong, H. Sun, Z. Ye, and Q. Zhang, "Heat extraction analysis for nonlinear heat flow in fractured geothermal reservoirs," *Computers and Geotechnics*, vol. 144, Article ID 104641, 2022.
[43] F. Xiong, H. Sun, Q. Zhang, Y. Wang, and Q. Jiang, "Preferential flow in three-dimensional stochastic fracture networks: the effect of topological structure," *Engineering Geology*, vol. 309, Article ID 106856, 2022.
[44] F. Miao, Y. Wu, Á. Török, L. Li, and Y. Xue, "Centrifugal model test on a riverine landslide in the Three Gorges Reservoir induced by rainfall and water level fluctuation," *Geoscience Frontiers*, vol. 13, no. 3, Article ID 101378, 2022.
[45] F. Miao, Y. Wu, Y. Xie, and Y. Li, "Prediction of landslide displacement with step-like behavior based on multialgorithm optimization and a support vector regression model," *Landslides*, vol. 15, no. 3, pp. 475–488, 2018.
[46] D. Song, Z. Chen, Y. Ke, and W. Nie, "Seismic response analysis of a bedding rock slope based on the time-frequency joint analysis method: a case study from the middle reach of the Jinsha River, China," *Engineering Geology*, vol. 274, Article ID 105731, 2020.
[47] Z. Chen, D. Song, C. Hu, and Y. Ke, "The September 16, 2017, Linjiabang landslide in Wanyuan County, China: preliminary investigation and emergency mitigation," *Landslides*, vol. 17, no. 1, pp. 191–204, 2020.
[48] F. Xiong, C. Zhu, G. Feng, J. Zheng, and H. Sun, "A three-dimensional coupled thermo-hydro model for geothermal development in discrete fracture networks of hot dry rock reservoirs," *Gondwana Research*, 2022.
[49] X. Cheng, Q. Zhang, Z. Zhang, Y. Zou, and G. Junjie, "Stress relief and stimulation of coal reservoir by hydraulic slotting," *Advances in Civil Engineering*, vol. 2021, Article ID 6664696, 13 pages, 2021.
[50] J. Zou, X. Hu, Y. Y. Jiao et al., "Dynamic mechanical behaviors of rock's joints quantified by repeated impact loading experiments with digital imagery," *Rock Mechanics and Rock Engineering*, vol. 55, no. 11, pp. 7035–7048, 2022.
[51] Z. C. Tang, Z. L. Wu, and J. Zou, "Appraisal of the number of asperity peaks, their radii and heights for three-dimensional rock fracture," *International Journal of Rock Mechanics and Mining Sciences*, vol. 153, Article ID 105080, 2022.